Mira Geoscience
...modelling the earth

Level 1, 39 Sherwood Rd
Toowong, QLD
4066
Tel : (07) 3720 8321
Fax : (07) 3870 2389

Cleveland Magnetic Modelling and AEM review

Elementos

Report no: 4655

August 2017

Mira Geoscience
...modelling the earth

Table of Contents

Mira Geoscience
...modelling the earth

1. Introduction

Mira Geoscience was commissioned by Elementos to carry out magnetic modelling over four prospective areas in the Cleveland area in Tasmania (Figure 1), an area prospective for Tin/Copper (cassiterite hosted in pyrrhotite). Elementos also requested modelling for a fifth area containing a dyke to be undertaken (Figure 1). For the latter, the aim is to derive a first pass representation of a dyke wireframe to help identify anomalies along the strike of the dyke which may be potentially associated with mineralisation.

The body of work also includes provision of time for assessment of public domain Hummingbird airborne electromagnetic (EM) data in the area, and plate modelling of any EM anomalies associated with the nominated targets.

The monoclinic form of pyrrhotite is magnetic, having susceptibility ~0.7 SI (Emerson et al.,1999). The hexagonal form is much less so, with susceptibility ~0.0015 SI. Monoclinic pyrrhotite is also an excellent electrical conductor, with a crystalline conductivity of >100,000 S/m. The conductivity of hexagonal pyrrhotite may be an order of magnitude less than that of the monoclinic form (Emerson et al., 2001). Pyrrhotite is typically amorphous and well-distributed, and this results in a high degree of electrical continuity in pyrrhotitic ores, which in turn results in high bulk electrical conductivities (albeit lower than the crystalline conductivity of pyrrhotite itself).

Other carbonate replacement tin deposits in Western Tasmania, such as Renison and Mt Bischoff are associated with anomalous magnetic and conductivity signatures. Cleveland is thought to have a subdued geophysical expression due to its relatively small size, and has not been well-characterised by the regional scale WTRMP electromagnetic and magnetic data (Morrison et al., 2003).

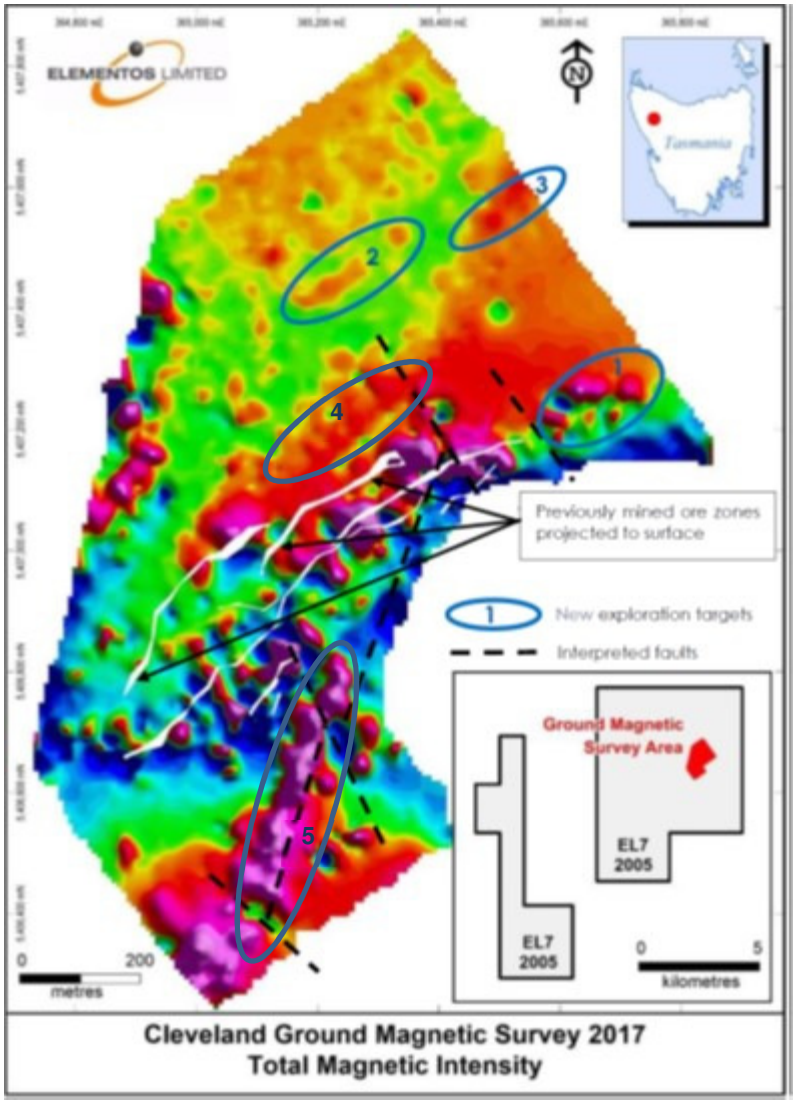

Figure 1: Supplied image of the Cleveland ground magnetic data TMI showing the locations of the four targets nominated for modelling and the dyke to the south.

2. Data compilation and assessment

The following data sets were supplied by Elementos:

- Ground magnetic data as a Geosoft database.
- LIDAR (DXF wireframes)
- Stopes and mine workings as DXFs.

Mira Geoscience acquired the public domain AEM survey. Details of the AEM survey are discussed in Section 5.

The stopes and mine workings were provided as a guide for general orientation of known mineralisation.

2.1. Magnetics

The survey totalled 33 line km at a 30m line spacing, covering an area spanning ~1200m E-W and ~1600m N-S (Figure 1).

Visual inspection of the magnetics data confirmed the data quality issues that that Elementos indicated existed in the data set (primarily due to rugged terrain), both in terms of Total Magnetic Intensity and GPS altitude. Figure 2 illustrates the ground magnetic survey lines coloured by magnetic intensity positioned according to the GPS altitude.

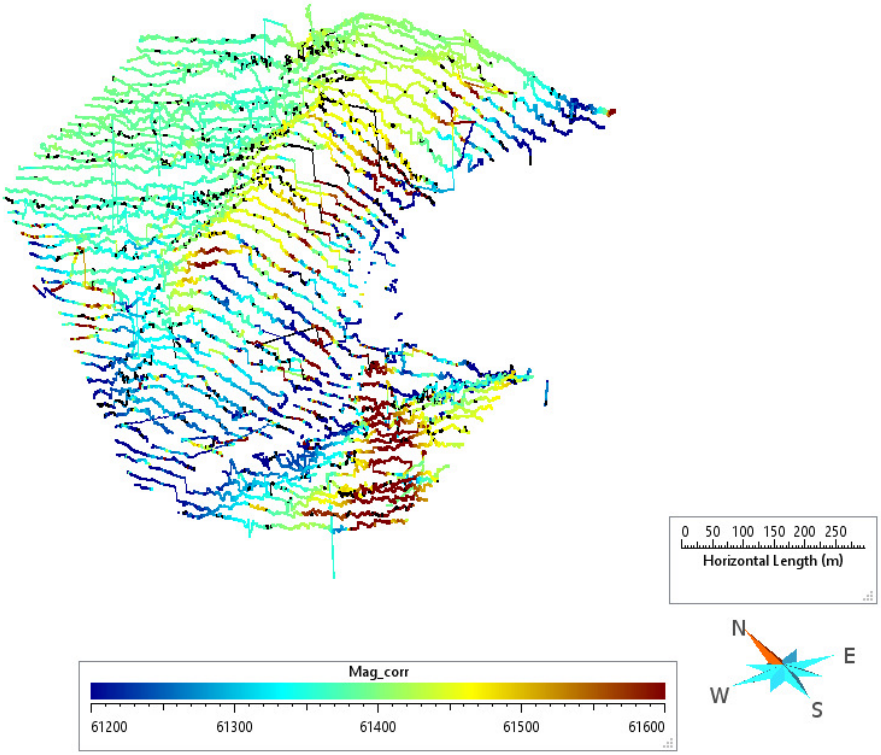

Figure 2: Perspective view of the ground magnetic survey located in 3D (vertical exaggeration =1). Measurements are coloured by the corrected magnetics (Mag_corr). Measurements coloured black represent Null values in the supplied data set (assumed to be spurious data that has already been removed).

Two mag channels existed in the data base; Mag_raw and Mag_corr. The Mag_corr data set was used for magnetic modelling.

By comparing the raw mag and the corrected mag in the supplied database, it was evident that some spurious measurements had already been removed from the corrected data. However, some outliers and inconsistencies in the data set still remained. Within the scope of this project, the entire data set was not re-processed or cleaned, bad data was simply removed as required to facilitate modelling.

The intensity and orientation of the earth's inducing field is required for magnetic modelling. The values were computed using the supplied co-ordinates, the date of the survey, and topography, using the Australian Geomagnetic Reference Field Computation provided online by Geoscience Australia.

The inducing field parameters are TF= 61649nT, Inclination=-71.688° and Declination=13.231°.

2.2. Elevation data

The ground magnetic data was supplied with GPS altitude data. The GPS measurements ranged from 128-585m, with an average of 391m and a standard deviation of 49m. The GPS altitude data contains spikes and irregular values (e.g. Figure 3).

LIDAR data was supplied, and due to the irregularity in the GPS measurements, the LIDAR was the assumed as the topographic reference for modelling.

Comparison of the original data elevations revealed a bulk shift with an average of 24.64m between the magnetic measurement locations and the LIDAR. This was inferred to be a difference in datum between the geoid and spheroid. There were also coherent localised deviations noted between the GPS data and the LIDAR as depicted by the height property in Figure 3 (11m standard deviation in differences). The local differences between magnetic measurement locations and the LIDAR were not investigated further in this project.

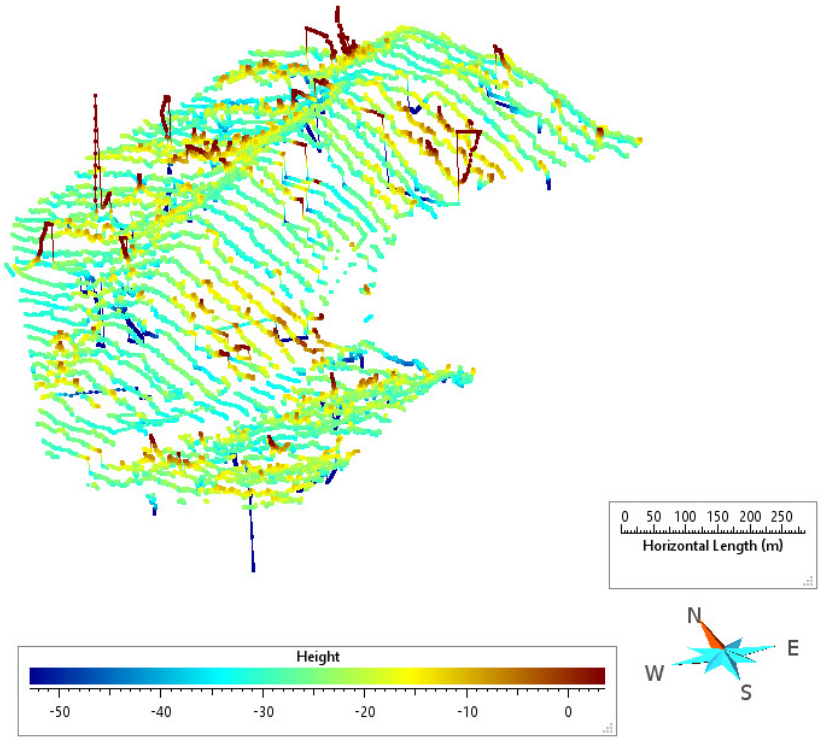

Figure 3: Magnetic data at GPS level showing height above LIDAR topography.

3. Magnetic Modelling methodology

The aim of the magnetic modelling was to model the geometry of magnetic domains that would explain the magnetic response inferred to be associated with possible targets.

Magnetic modelling comprised two key phases; magnetic modelling along profiles using simple (tabular) dipping bodies to explain the magnetic response, and magnetic modelling of 3D wireframes. In 3D, the wireframes were initially constructed based on profile modelling outcomes, then their shape adjusted to improve the fit between the measured and calculated response over the body. No geological or petrophysical constraints were supplied to constrain magnetic modelling. A constant magnetic susceptibility was assumed for each nominated area.

The final product of modelling is a 3D wireframe for each of the selected targets.

Profile modelling was completed using Windisp (Scientific Computing). All 3D modelling was carried out in Gocad Mining Suite (Paradigm and Mira Geoscience) using VPmg (Mira Geoscience) for magnetic modelling. Appendix A provides an overview of the VPmg modelling software.

3.1. Data preparation:

Magnetic modelling used the corrected magnetic data (Mag_corr) from the Geosoft database draped 1.5m above the LIDAR.

During modelling, isolated spikes in the corrected mag data were removed, and repeat lines were also removed (favouring the line that had the most coherent representation of the anomaly represented on adjacent lines).

A key consideration for magnetic modelling is isolating the response associated with the selected targets from the magnetic response of the surrounding (background) geology. Various techniques were tested during this component of work.

The final method employed for isolating the background response in this project was to grid the data, filter the response (using a combination of median filtering to remove outliers, then an averaging filters across the grid), mapping the filtered data back onto the ground mag lines and subtracting it from the corrected magnetics. The supplied corrected magnetics, low pass filtered response, and residual response are illustrated in Figure 4.

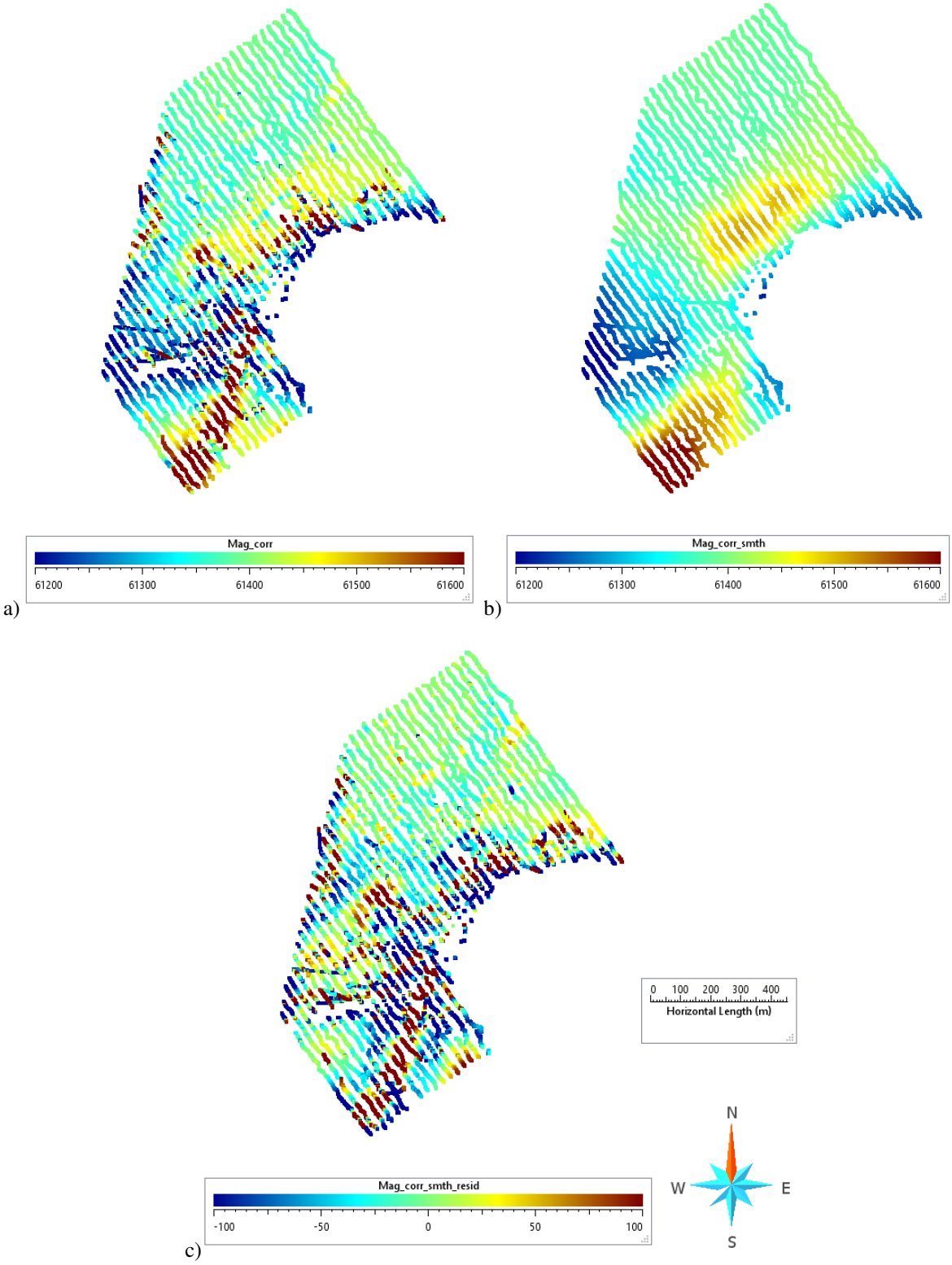

Figure 4 ***Illustrates a) the supplied magnetics (Mag_corr), b) the approximate background response and c) the supplied magnetics with the background response removed. The colour stretch in c) is difficult to optimise for reporting purposes as the target responses in the north are weak compared to the dyke response to the south. The illustrated responses are included in the deliverables in ascii format.***

This method of preparing the data provided a more robust separation of magnetic signal than simple trend removal, or filtering along lines. The recommended approach for dealing with magnetic response of background geology is to explicitly model the background geology.

4. Magnetic modelling results

The outputs from the magnetic modelling are 3D modelled domains (wireframes) that explain the magnetic response associated with the selected targets. An overview of the modelled wireframes is illustrated in Figure 5 shown with respect to the LIDAR topographic surface.

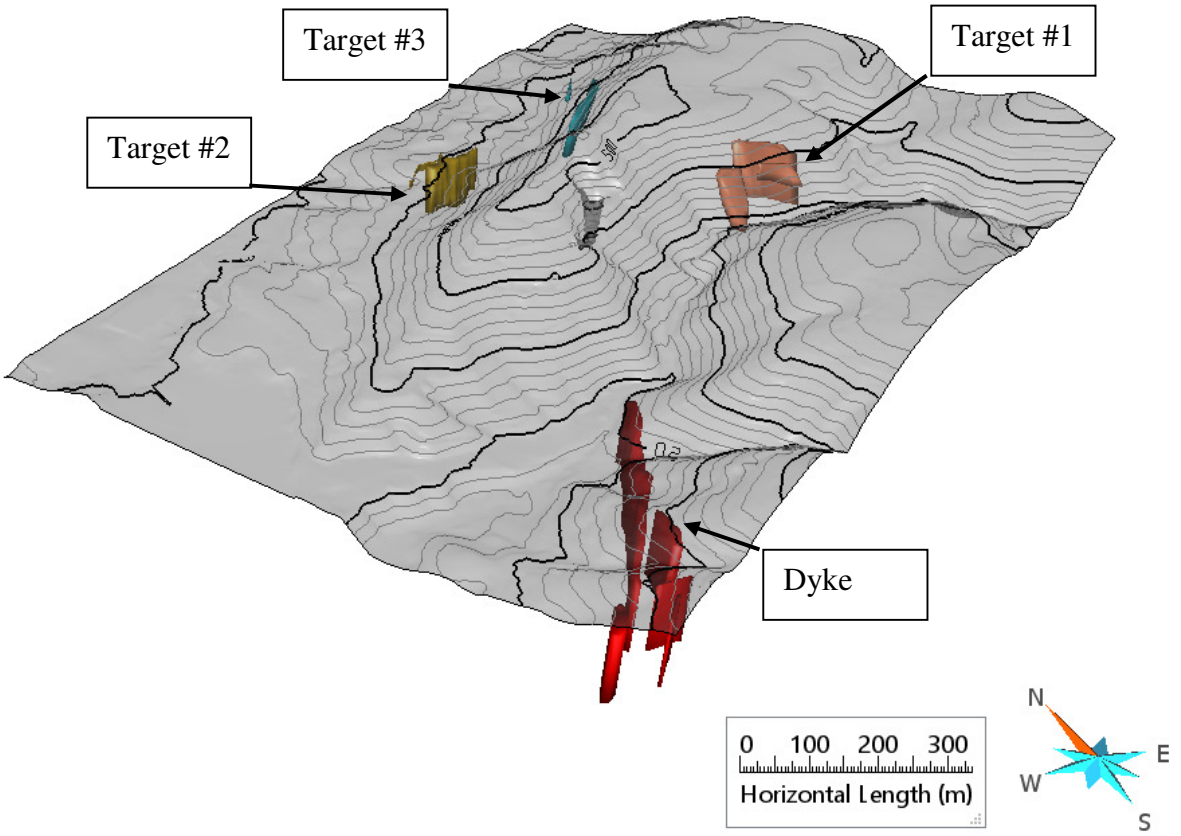

Figure 5: Perspective view of the transparent topography surface with contours at 10m intervals, showing the locations of the modelled targets.

The modelled wireframes are provided in DXF format and also as part of a Geoscience ANALYST project (a free 3D visualization software provided by Mira Geoscience). The compiled Geoscience ANALYST project also contains comparisons of the measured and calculated magnetic responses.

Magnetic modelling results are presented for each target in the following subsections. While the results are best visualized in 3D, within this report the modelled wireframes are illustrated with a perspective 3D view, a plan view with observed and calculated data shown above the model, a horizontal depth slice through the models and cross-sections to clearly depict the locations of the modelled domains.

4.1. Target 1

Three wireframes are used to model the prominent magnetic response associated with this selected target (Figure 6). The two larger domains explain the majority of the response, but the thin magnetic filament (towards the SE) is included to explain the narrow magnetic high observed across two of the survey lines.

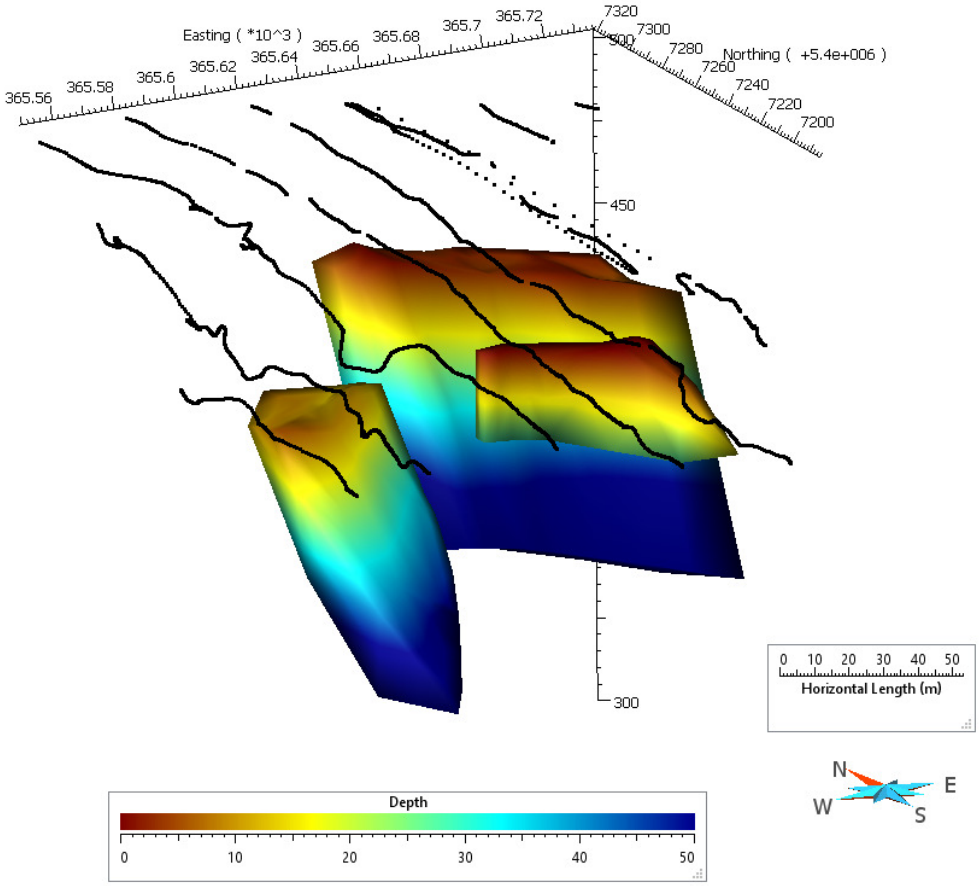

Figure 6: Perspective view of the modelled domains for Target 1 coloured by depth. The locations of the magnetic data in 3D are illustrated as black points.

A plan view representation of the modelled wireframes with measured and calculated magnetic responses is shown in Figure 7. Inconsistent repeat measurements towards the East are excluded from the illustration. For a simplified model, the correspondence between the observed and measured data is reasonable, particularly in view of data quality and uncertainty

in the magnetic response. There is a pronounced magnetic low immediately north of the SW magnetic body which the modelling could not explain; this response is considered spurious.

Each of the three wireframes modelled in this area has a susceptibility of 0.03SI.

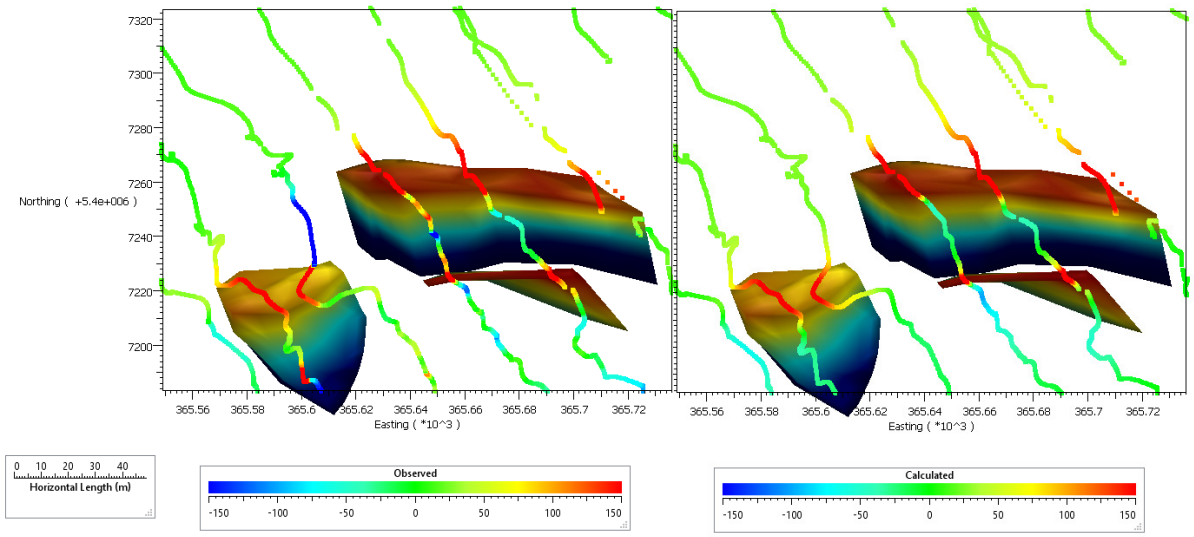

Figure 7: Map view of the modelled domains for Target 1 coloured by depth. Profiles are coloured by TMI, and compare the measured TMI used for modelling (left) and the calculated TMI response of the modelled wireframes (right).

Additional plan and horizontal sections of the modelled domains are provided below (Figure 8 and Figure 9). Depth to the top of the wireframes are illustrated in Figure 6 and exhibit values that are essentially outcropping to ~15m depth. The depth extent (down dip) of the two larger domains is ~70m, and is < 25m for the thin domain to the SE. The two major bodies are ~10-15m wide. The thin body to the south is only ~2-3m wide.

Of the two major domains, the dip of the SW body is 60 degrees toward the SE (145 degrees) while the larger eastern body has been modelled with a 70 degree dip towards the S-SSW. The thin filament to the SE exhibits a near vertical dip towards the west, but dips towards the south further east. The thin body in fact dips slightly to the north as is evident in Section 2 of Figure 9b below.

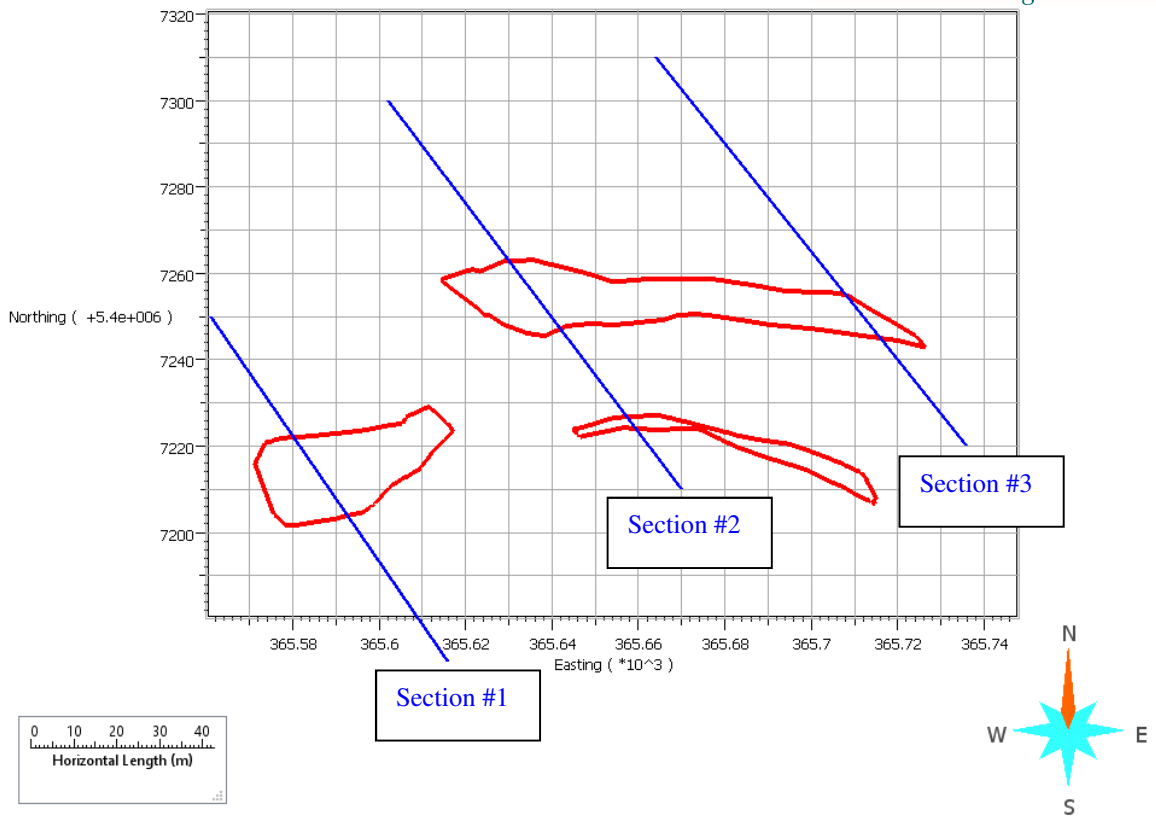

Figure 8: Map view illustration of a 20m depth slice through the modelled domains for Target 1. Blue lines represent the locations of cross-sections through the modelled domains shown below.

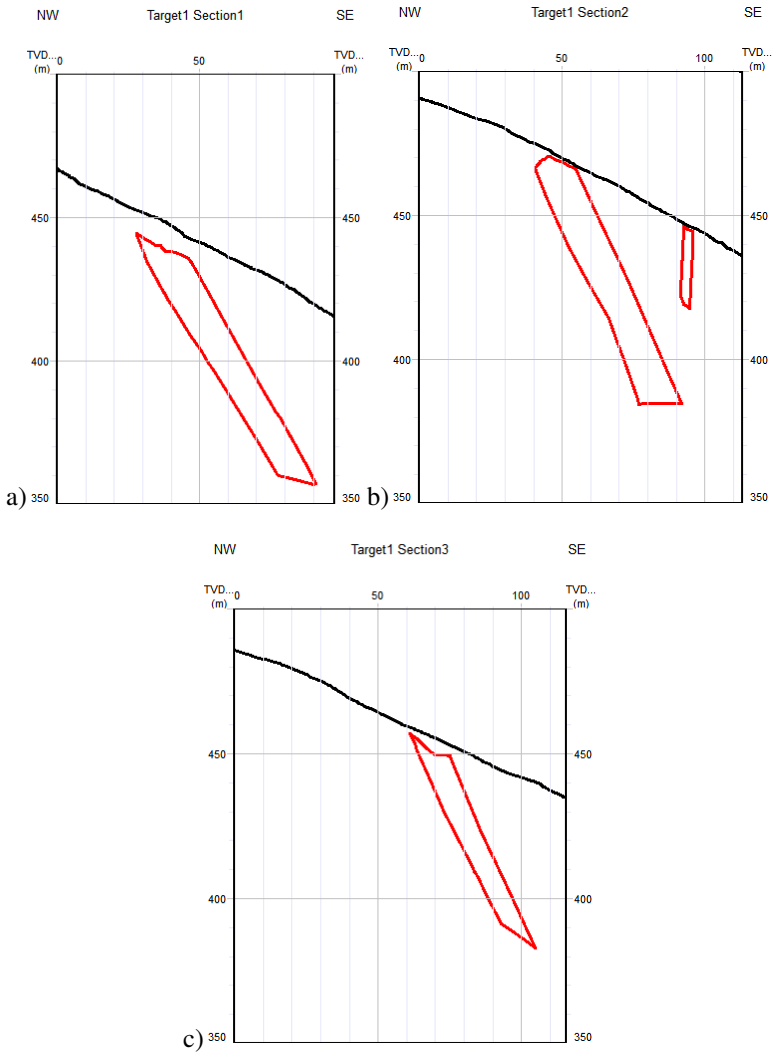

Figure 9: Cross Sections through the modelled domains for Target 1. Locations of cross-sections are shown in Figure 8 and end points are documented in the table below.

Eastings and northings of end points of the cross-section lines are:

Cross-section1:	365561, 5407250	365616, 5407170
Cross-section2:	365602, 5407300	365670, 5407210
Cross-section3:	365664, 5407310	365736, 5407220

The locations of lines are provided in DXF format in the digital deliverables.

4.2. Target 2

The magnetic response associated with this target is essentially explained by one magnetic domain, however a small magnetic filament to the SW was also included to account for a subtle magnetic signature noted in the data. The two wireframes are shown in Figure10 coloured by depth.

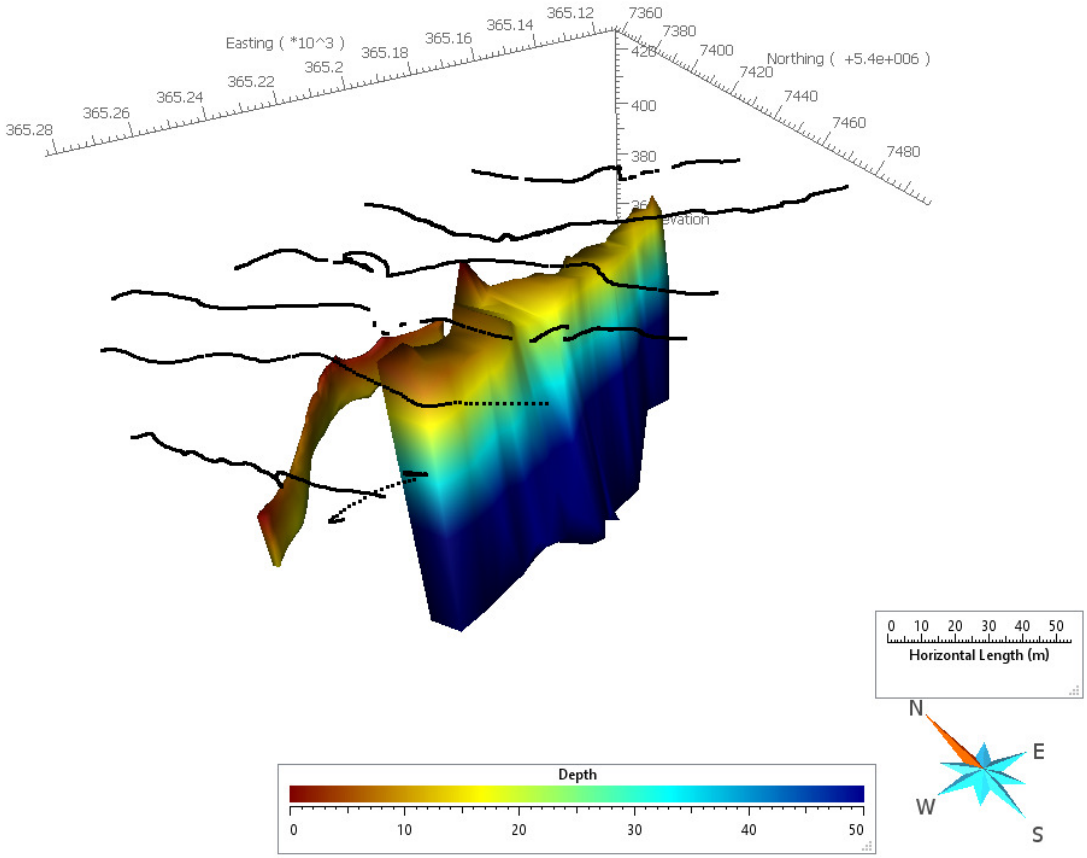

Figure10: Perspective view of the modelled domains for Target 2 coloured by depth. The locations of the magnetic data in 3D are illustrated as black points.

A plan view representation of the modelled wireframes with measured and calculated magnetic responses is shown in Figure 11. The magnetic high response over the anomaly is well represented in the recomputed response. In this case, there are notable background variations in the measured response on either side of the main magnetic anomaly that are not explained with the modelled target geometry.

Each of the two wireframes modelled in this area has a susceptibility of 0.005SI.

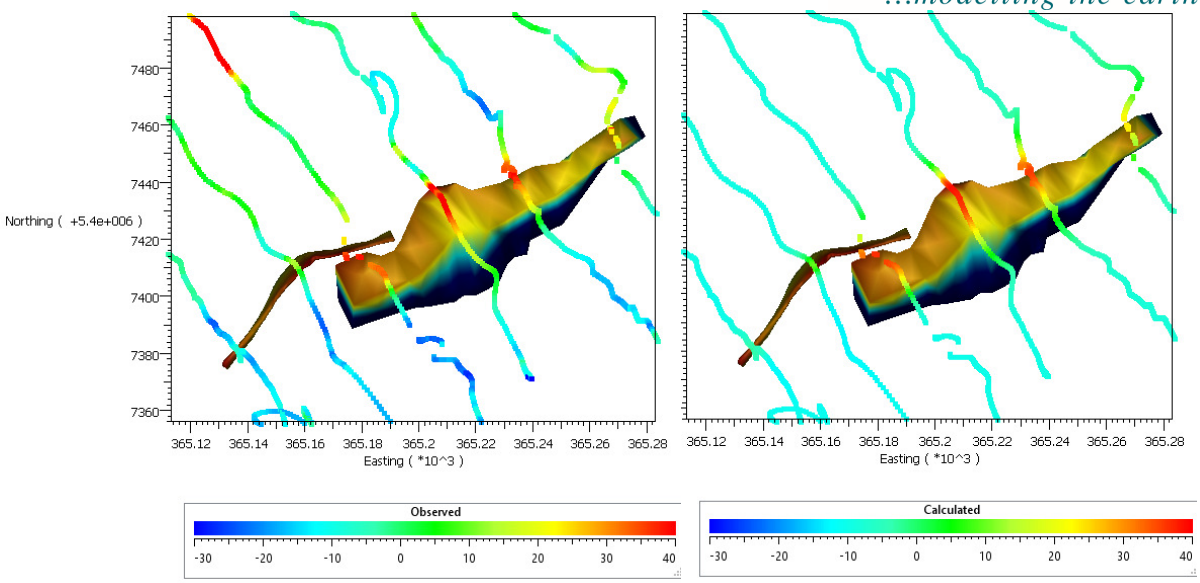

Figure 11: Map view of the modelled domains for Target 2 coloured by depth. Profiles are coloured by TMI, and compare the measured TMI used for modelling (left) and the calculated TMI response of the modelled wireframes (right).

Additional plan and horizontal sections of the modelled domains are provided below (Figure 12 and Figure 13).

Depth to the top of the wireframes are illustrated in Figure10. The main wireframe has depths to the top between ~5-15m. There is a narrow peak on the northern edge of the main body near the center which was modelled to explain a narrow feature in the measured TMI data (Figure 13b). These thin protrusions from the main body were supported by profile modelling, to explain narrow magnetic responses superimposed on the response of the main body.

The thin magnetic filament towards the SW is practically outcropping in places with a maximum depth to top of ~9m. The thin magnetic filament only extends to a maximum depth of ~25m. The depth extent (down dip) of the larger domain is ~75m. The major body varies in width from profile to profile, but is generally between 8-17m wide. The thin body to the south is only ~2-3m wide.

The major domain is dipping S-SSE with dips ranging from about 72-90 degrees. The thin filament is dipping towards the north, with dips generally between 75 and 85 degrees.

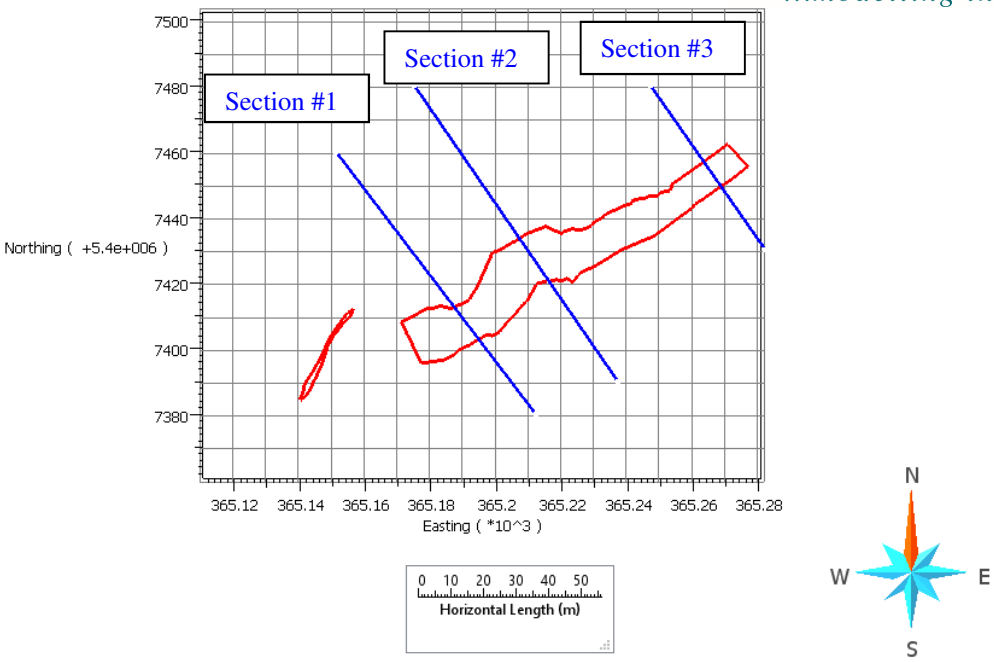

Figure 12: Map view illustration of a 20m depth slice through the modelled domains for Target 2. Blue lines represent the locations of cross-sections through the modelled domains shown below. Note: the thin filament towards the SW is only partially zone because portions of it do not exist at 20m depth.

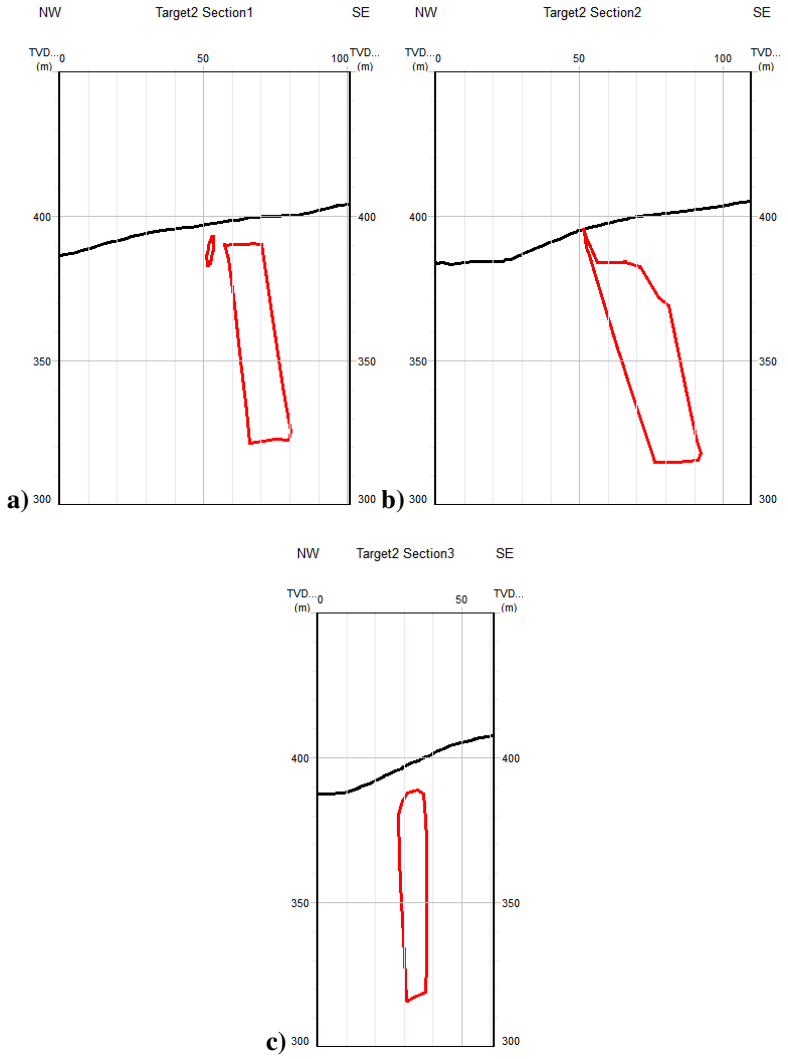

Figure 13: Cross Sections through the modelled domains for Target 2. Locations of cross-sections are shown in Figure 12 and end points are documented in the table below.

Eastings and northings of end points of the cross-section lines are:

Cross-section1:	365151 5407460	365212 5407380
Cross-section2:	365175 5407480	365237 5407390
Cross-section3:	365247 5407480	365282 5407430

The locations of lines are provided in DXF format in the digital deliverables.

4.3. Target 3

The magnetic response associated with this target is essentially explained by one magnetic domain, however a small magnetic filament to the north was also included to account for a subtle magnetic signature noted in the data. The two wireframes are shown in Figure 14 coloured by depth.

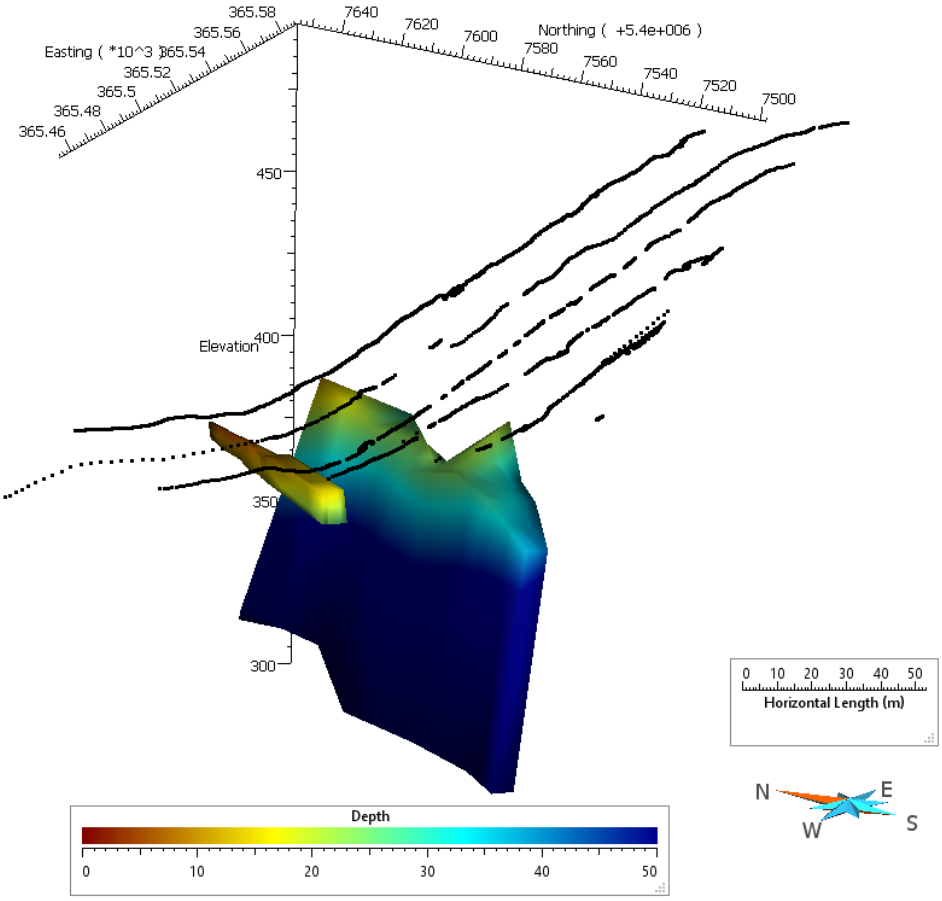

Figure 14: Perspective view of the modelled domains for Target 3 coloured by depth. The locations of the magnetic data in 3D are illustrated as black points.

A plan view representation of the modelled wireframes with measured and calculated magnetic responses is shown in Figure 15. As for target #2, the magnetic high response over the anomaly is well represented in the recomputed response, but there are notable background variations in the measured response that are not explained with the modelled target geometry.

Each of the two wireframes modelled in this area has a susceptibility of 0.015SI.

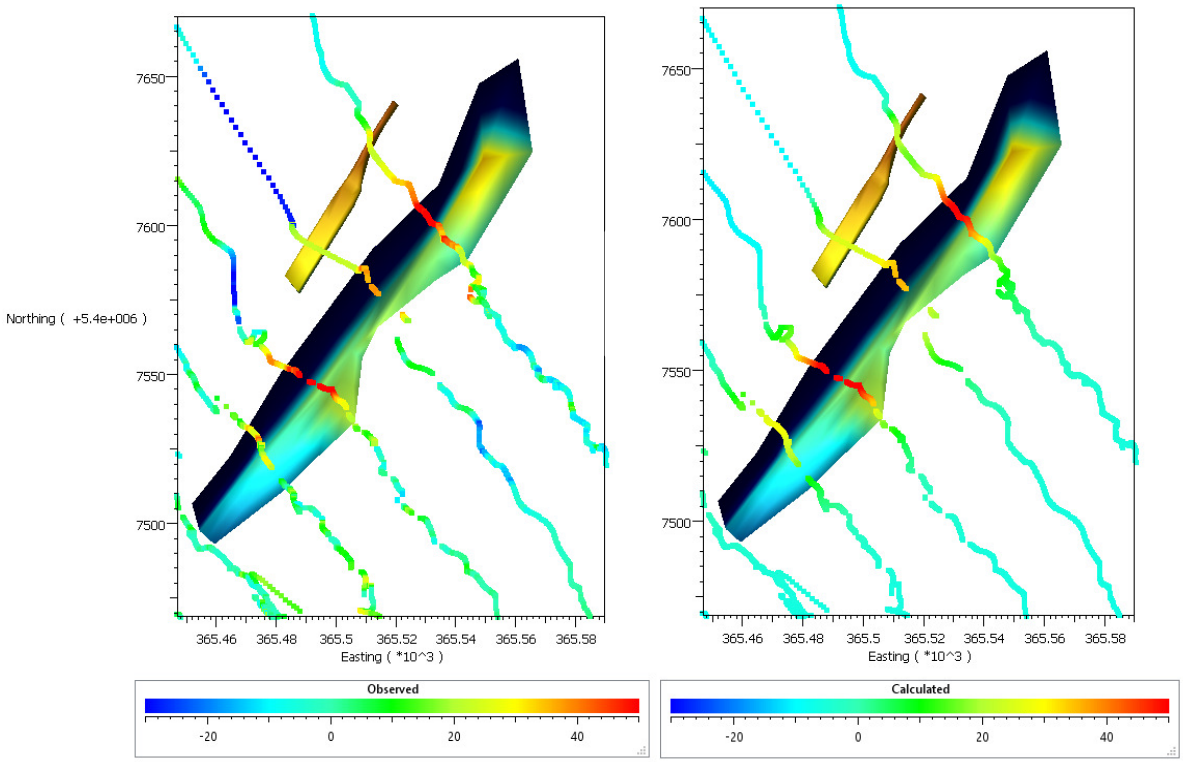

Figure 15: Map view of the modelled domains for Target 3 coloured by depth. Profiles are coloured by TMI, and compare the measured TMI used for modelling (left) and the calculated TMI response of the modelled wireframes (right).

Additional plan and horizontal sections of the modelled domains are provided below (Figure 16 and Figure 17).

Depth to the top of the wireframes are illustrated in Figure 14. The main wireframe has depths to top between ~20-40m. The northern end of the model is actually shallower than 20m, but this is simply an extension of the domain, and no magnetic data exists over the northern-most extent of the model. That is, there is no data to support the very thin northern end of the magnetic body.

As for target #2, there is a narrow peak on the edge of the main body near the center which was modelled to explain a narrow feature in the measured TMI data. The thin magnetic filament is practically outcropping in places with a maximum depth to top of ~9m. The thin magnetic filament is ~5m wide at its southern extent, and 2-3m wide towards the north, with limited depth extent (<10m). The depth extent (down dip) of the larger domains is ~75m. The major body varies in width from profile to profile, but is generally within 7-13m wide.

The major domain is dipping NW-NNW at approximately 80 degrees. Towards the NE end a better fit to the data was obtained by allowing the dip to shallow slightly to 70 degrees. It is important to note that there is no magnetic data over the north-eastern most part of the magnetic domain. The thin filament is basically vertical, with dips ranging from about 80-90 degrees.

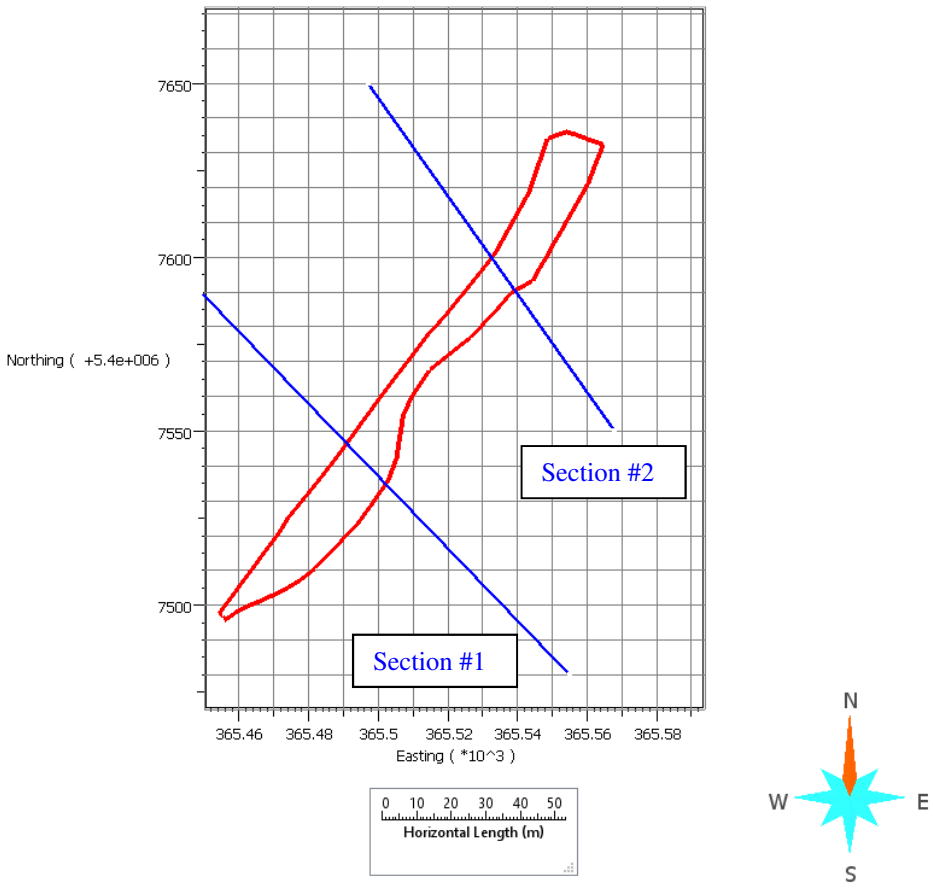

Figure 16: Map view illustration of a 40m depth slice through the modelled domains for Target 3. Note that the depth extent of the smaller body is entirely < 20m. Blue lines represent the locations of cross-sections through the modelled domains shown below.

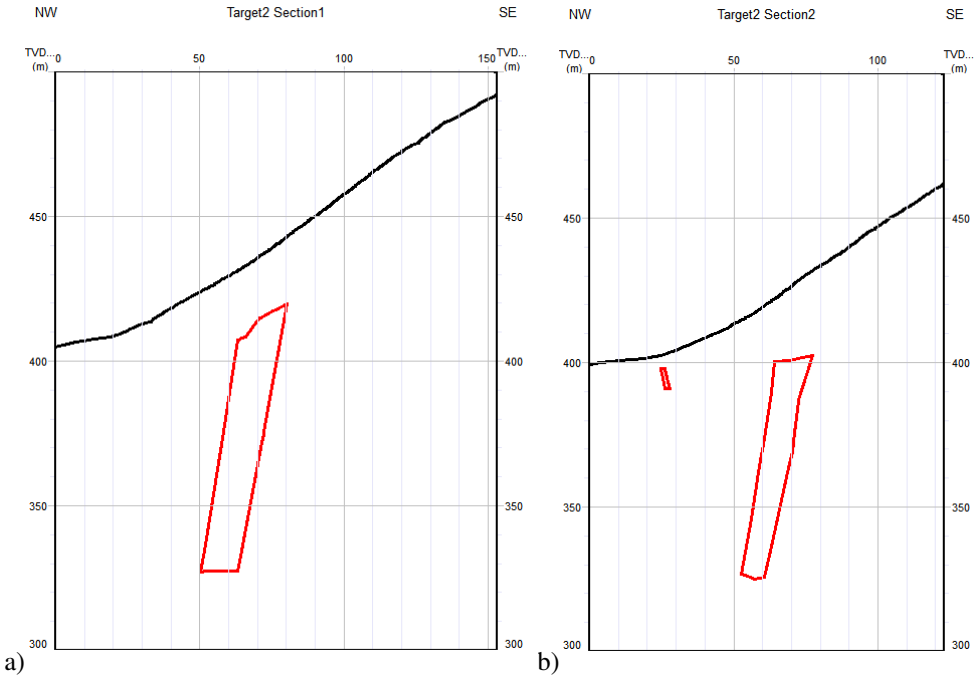

Figure 17: Cross Sections through the modelled domains for Target 3. Locations of cross-sections are shown in Figure 16 and end points are documented in the table below.

Eastings and northings of end points of the cross-section lines are:

Cross-section 1:	365449, 5407590	365555, 5407480
Cross-section2:	365497, 5407650	365568, 5407550

The locations of lines are provided in DXF format in the digital deliverables.

4.4. Target 4

The magnetic response associated with target #4 was investigated and it was unclear whether there was an anomaly associated with a discrete target to model.

It is inferred that the original identification of target #4 (purple outline in Figure 18) was based on images of the magnetic survey data that have been histogram equalized and possibly even illuminated or shaded. Closer inspection of the ground magnetic data in profile view and map view reveal a prominent negative magnetic anomaly (e.g. dark grey outline in Figure 18) along the topographic ridge. This negative response accentuates the appearance of a positive 'anomaly' of interest immediately to the NW, particularly when a grid is histogram equalized.

Arguably, if the negative anomaly was removed, the response to the north may not have been identified as a target.

Further to this, direct inspection of the profiles revealed many data drop outs along several of the lines in this area, that would adversely affect modelling.

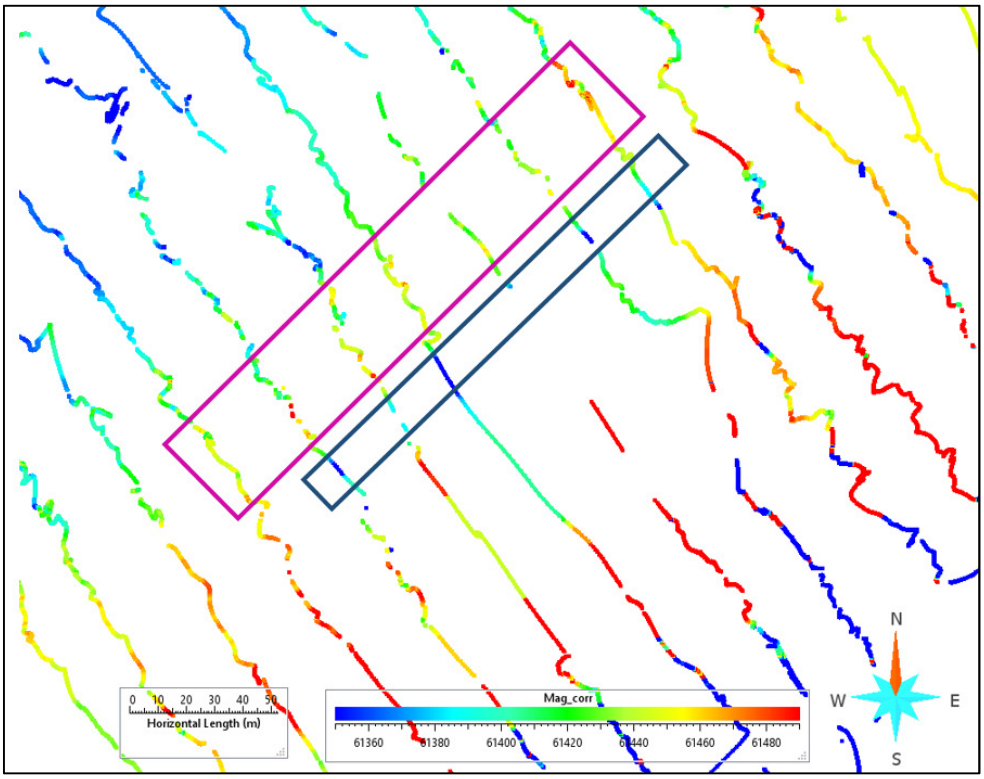

Figure 18: Illustrates the corrected magnetic data over "Target #4". The dark grey outline highlights the negative anomaly, whereas the purple outline represents the area where the subtle positve magnetic anomaly arguably exists.

To exhaust possibilities, various modelling efforts were quickly investigated to assess if a positive magnetic susceptibility distribution could explain the measured magnetic signature and the highs on either side. These conceptual models included a) a low magnetic susceptibility zone along the cap of the ridge in an otherwise magnetically susceptible host and b) thin shallow dipping sheets almost parallel to the topography to produce a low along the top of the ridge.

Neither of these efforts provided sufficient encouragement to suggest that these were plausible explanations of the magnetic low response. Unfortunately, within the budget allocated for this

project, it was not possible to pursue this further, or document these investigations fully in this report.

The final hypothesis is that there is a sub-vertical, negatively magnetized dyke-like feature near the top of the ridge, ~5-10m across. It is possible that the negative magnetic feature may be associated with data quality issues, but the fact that is exists across multiple lines suggests it is real.

Mira Geoscience can discuss possible further investigations as an extension to this work if Elementos is interested in pursuing this target.

4.5. Dyke modelling and assessment

The primary aim of the dyke modelling was to identify irregularities associated with the dyke. Assessment of the dyke was undertaken through direct inspection of the magnetic response, 3D modelling of wireframes to explain the magnetic response of the dyke, and assessment of remaining unexplained magnetic response.

Due to the length of dyke, some simplified assumptions were made to expedite wireframe modelling. For example, the dip of the dyke was assumed to be vertical along its entire extent, with a constant depth extent (100m). These assumptions allowed the aims of the dyke modelling to be adequately met within the time available for the project. Several susceptibilities values were tested and a susceptibility of 0.1 SI was used. Adjusting the position and shape of the top of the dyke was the key mechanism for explaining the measured magnetic response.

This section will outline the dyke 3D modelling result (as per the previous targets), then conclude with a discussion of irregularities associated with the dyke.

Dyke wireframe modelling

The magnetic response associated with the dyke is reasonably explained with 5 modelled wireframes. The wireframes are shown in Figure 19 coloured by depth.

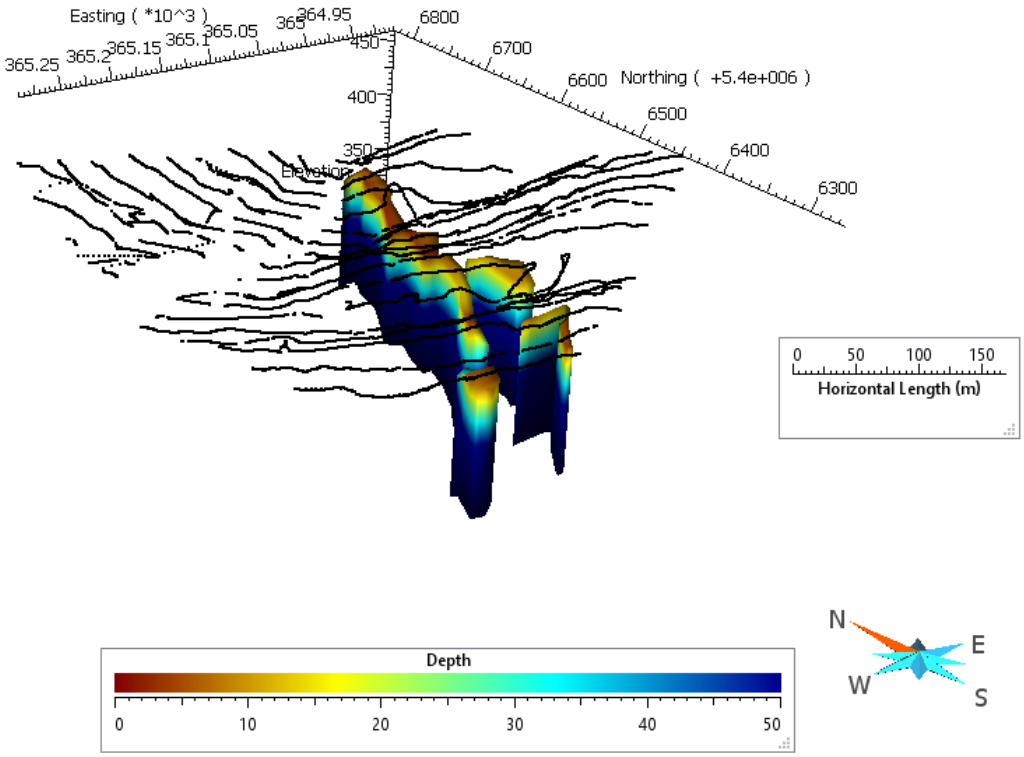

Figure 19: Perspective view of the modelled domains for the dyke coloured by depth. The locations of the magnetic data in 3D are illustrated as black points.

A plan view representation of the modelled dyke wireframes with measured and calculated magnetic responses is shown in Figure 20. The overall fit is considered acceptable given the simplifying assumptions made for modelling the dyke.

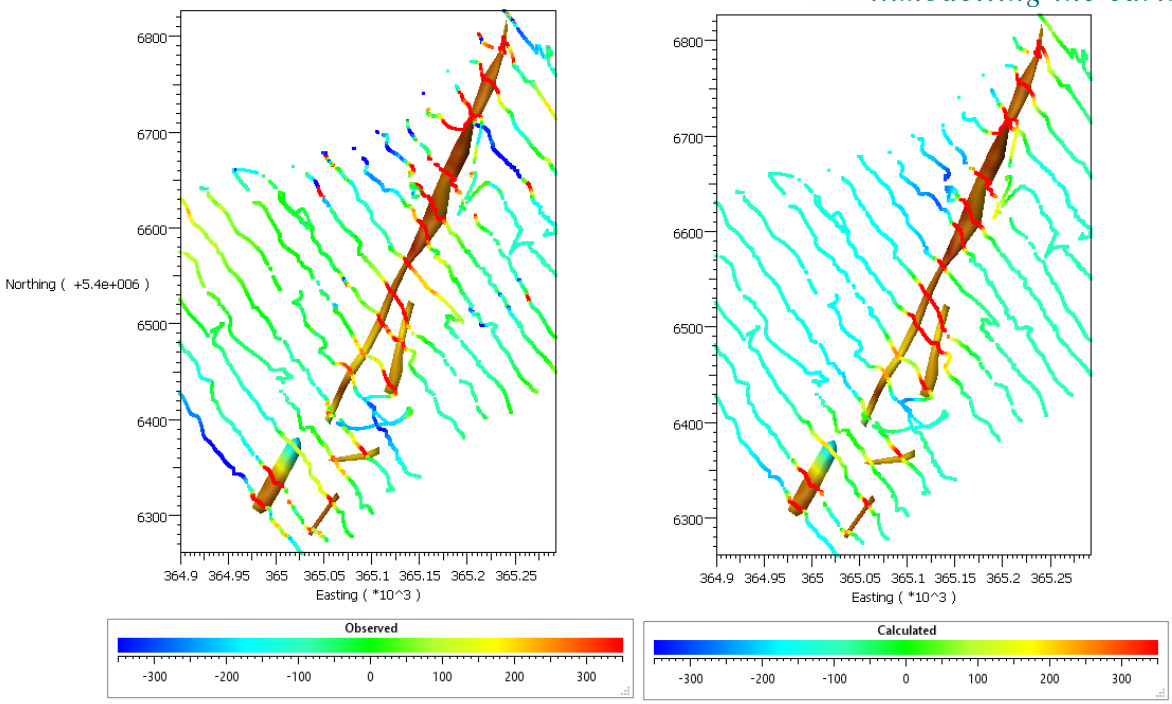

Figure 20: Map view of the modelled domains for the dyke coloured by depth. Profiles are coloured by TMI, and compare the measured TMI used for modelling (left) and the calculated TMI response of the modelled wireframes (right).

Additional plan and horizontal sections of the dyke domains are provided below (Figure 21 and Figure 22).

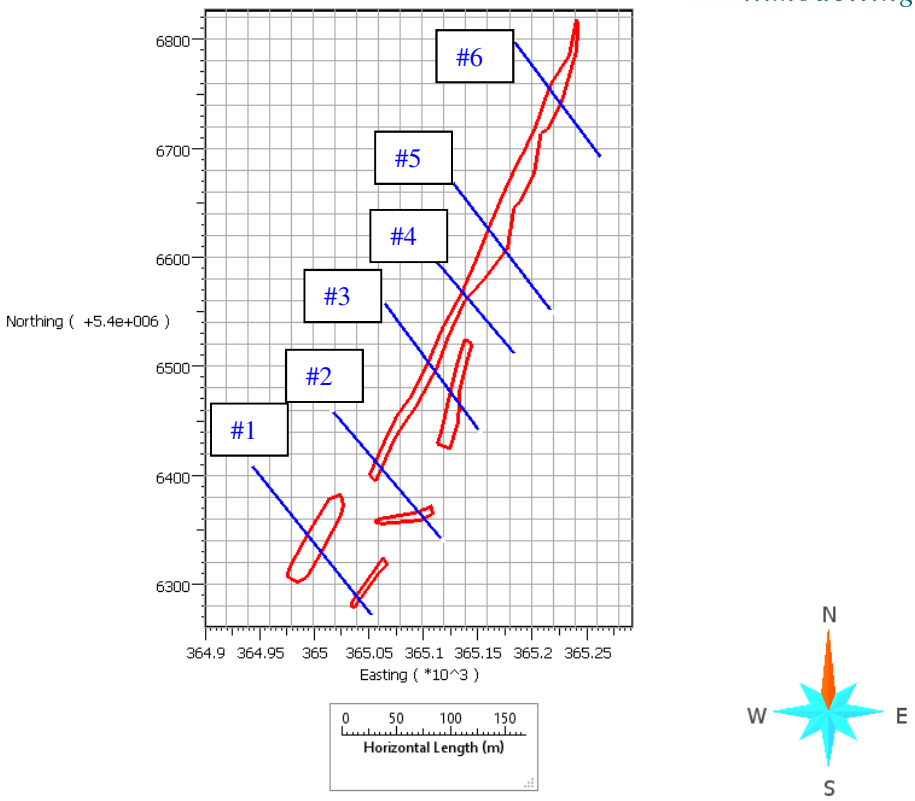

Figure 21: Map view illustration of a 40m depth slice through the modelled domains for the dyke. Blue lines represent the locations of cross-sections through the modelled domains shown below.

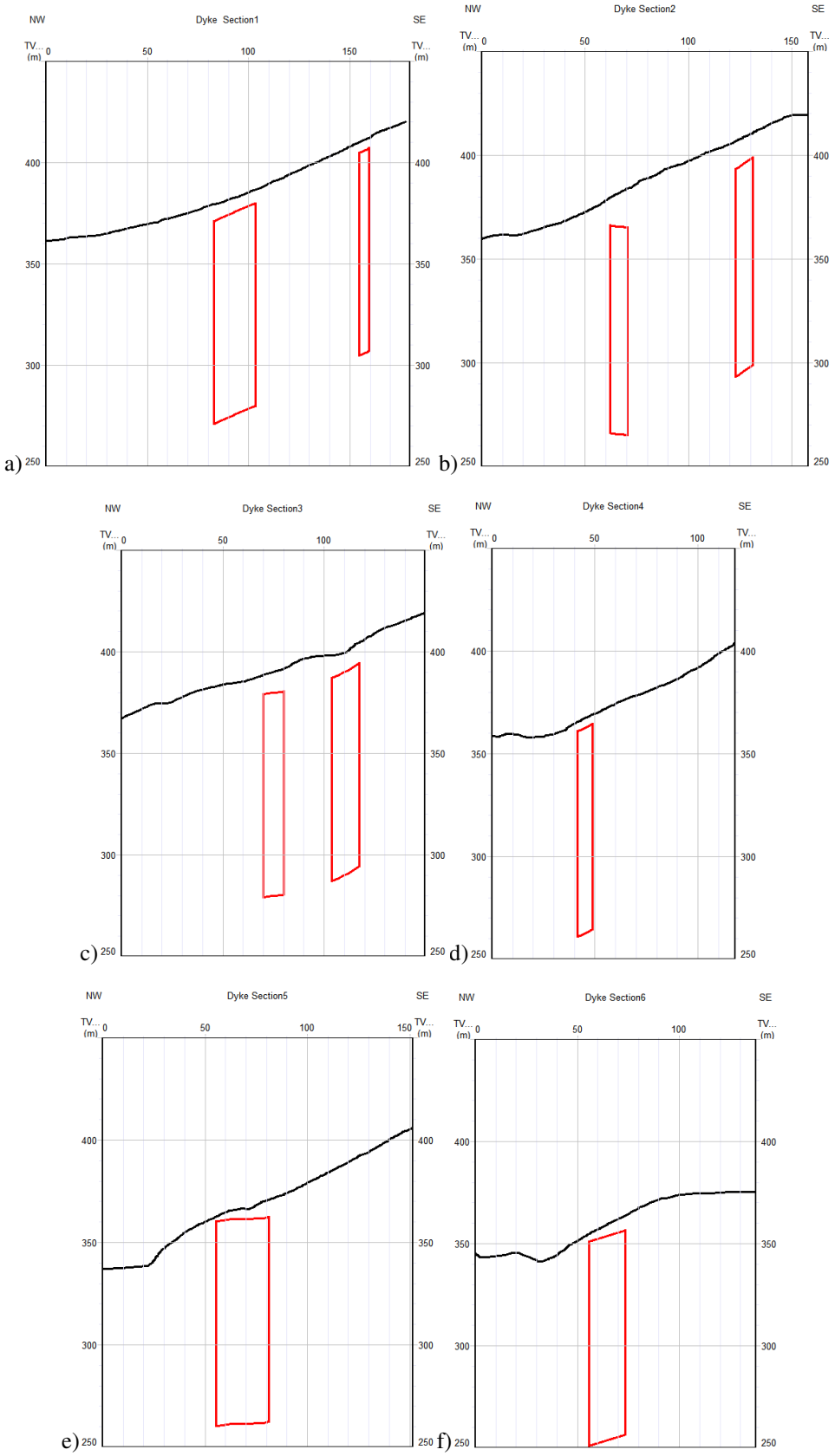

Figure 22: Cross Sections through the modelled domains for the dyke. Locations of cross-sections are shown in Figure 21 and end points are documented in the table below.

Eastings and northings of end points of the cross-section lines are:

Cross-section 1	364942 5406410	365054 5406270
Cross-section 2	365016 5406460	365118 5406340
Cross-section 3	365063 5406560	365152 5406440
Cross-section 4	365109 5406600	365185 5406510
Cross-section 5	365126 5406670	365218 5406550
Cross-section 6	365182 5406800	365264 5406690

The locations of lines are provided in DXF format in the digital deliverables.

Assessment for irregularities along the dyke.

Assessment of irregularities along the dyke was based on direct inspection of the magnetic response, the shape of the 3D wireframes, and assessment of remaining unexplained magnetic response (data misfit). Assessment of the data misfit of the modelling serves to identify possible irregularities and variations in dip e.g. it was inferred from inspection of the misfit that the northern end of the dyke may be dipping slightly towards the WNW.

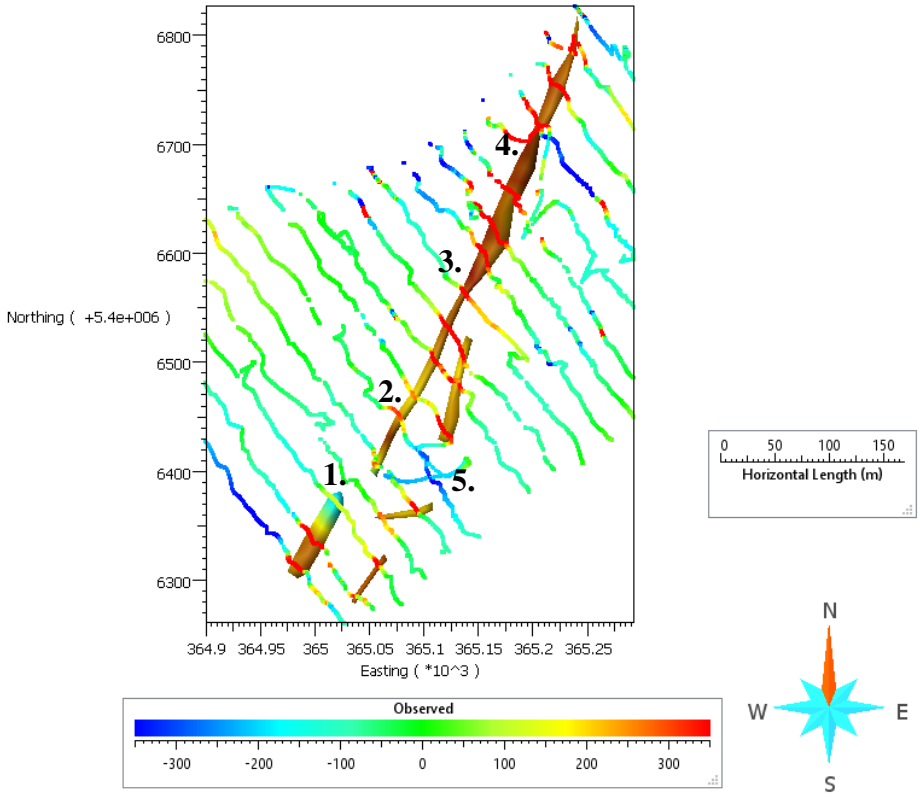

Figure 23: Illustrates the measured dyke response shown relative to the position of the modelled dykes. Numbered annotations relate to noted ireggularities listed below.

Key features interpreted to be associated with irregularities include the following:

1. Absolute break/discontinuity along main body of dyke.
2. There is a notable thinning of the dyke north of this continuity.
3. The dyke thickness increases north of the point annotated by #3, and based on inspection of the residual response, may in fact be dipping 10-20 degrees towards the WNW further north of this point. This would make this juncture in the dyke an irregularity.
4. Localised thinning and swelling of the dyke towards the north would also be inferred as irregularities.
5. 3 smaller domains SE of main dyke body may themselves be considered irregularities (if not possible targets).

It is important to consider variations in data quality along the strike of the dyke when following up the noted irregularities.

5. Hummingbird AEM assessment

The Cleveland area was covered by the regional-scale Western Tasmania Regional Minerals Program regional geophysical survey. This included frequency-domain electromagnetics (Hummingbird), flown on east-west lines at 200 m line spacing. Nominal height of the EM sensor above ground was 30 m, although this was much higher in places due to vegetation and steep terrain. The Hummingbird system employs five transmitter-receiver coil pairs, three of which are in a horizontal coplanar (CP) geometry and two in a vertical coaxial (CX) geometry. The CP data was measured at frequencies of 34,000 Hz, 6,600 Hz, and 880 Hz, and the CX at 7,004 Hz and 980 Hz. Data from the CX coil pairs show higher lateral resolution (ie more sharply defined anomalies) than the CP, and the CX geometry and is also better coupled to subvertical conductors than the CP. Depth of investigation increases as frequency decreases: the 34,000 Hz data thus provides the shallowest information, and the 880 Hz data the deepest. Poor geological conductors will show strong response at higher frequency, but little or none at low frequency, whereas good conductors exhibit strong responses at the lower frequencies. The inphase component of the Hummingbird response at low frequency is also sensitive to magnetic permeability, provided the ground is not highly conductive. Shallow magnetic features within the depth of investigation of the system produce characteristic negative inphase responses in the low-frequency CP data.

Pyrrhotite is highly electrically-conductive, and its monoclinic form is also magnetic. Pyrrhotite is amorphous, and rocks containing relatively high amounts of this suphide (greater than say 5 wt%) exhibit high electrical continuity which in turn results in high bulk electrical conductivity.

Other carbonate replacement tin deposits in Western Tasmania, such as Renison and Mt Bischoff are associated with anomalous magnetic and conductivity signatures. Cleveland is thought to have a subdued geophysical expression due to its relatively small size, and has not been well-characterised by the regional scale WTRMP electromagnetic and magnetic data (Morrison et al., 2003).

Figure 24 shows the 880 Hz CP apparent conductivity grid at Cleveland, with the approximate positions of the Elementos magnetic targets superimposed. The extensive conductor just to the west of the ground magnetic survey area corresponds to outcrop/subcrop of the Whyte River

mafic/ultramafic complex (Reid, 2003). There is only one weak conductor evident in the ground magnetic survey area, which coincides with the northeastern end of the dyke target. The conductor is located in an area of low topography (Figure 26), and is most likely to be associated with alluvium or weathering rather than to mineralisation which would be expected to be strongly conductive. High conductivities around Targets 2 and 3 are likely to be the flanks of the large anomaly associated with the Whyte River complex. Although only the 880 Hz data is included here, no conductors associated with any of the magnetic targets are evident in any of the higher frequency electromagnetic data.

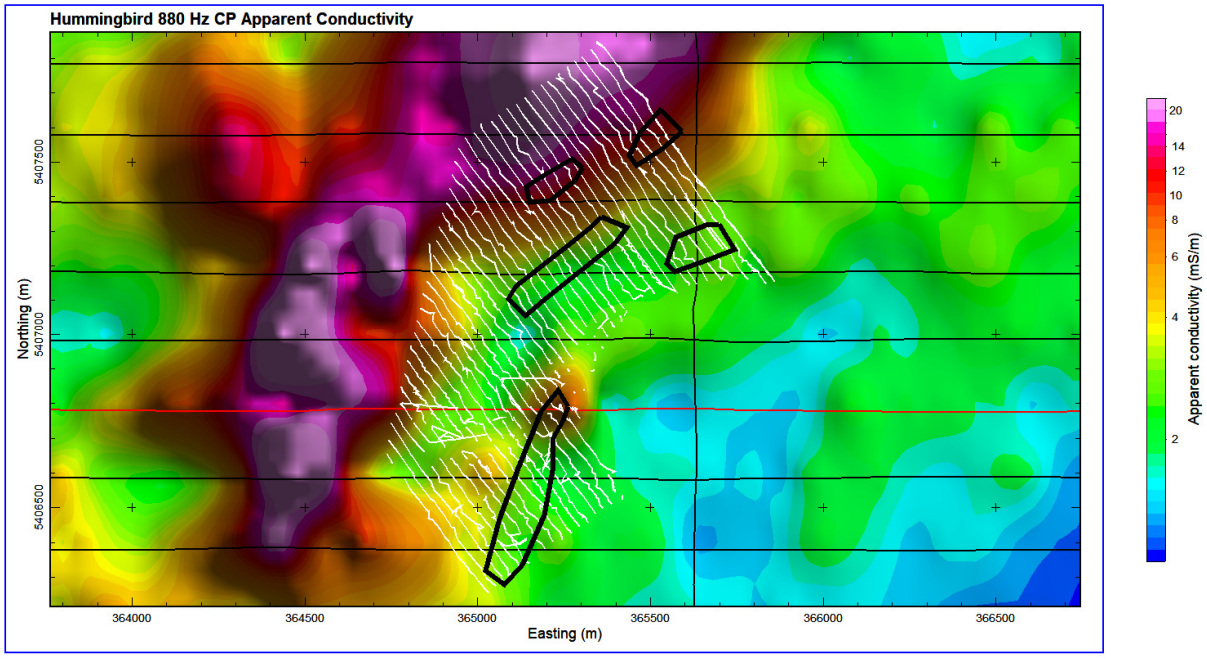

Figure 24 Grid of Hummingbird 880 Hz CP Apparent conductivity at Cleveland. The ground magnetic survey lines are shown in white. The black polygons show the rough outlines of the five targets identified by Elementos (Figure 1). Flightline 10531 (see Figure 27) is highlighted in red.

Figure 25 shows the WTRMP helimagnetic data at the same scale at Figure 24, and is included for the purposes of comparison. The aeromagnetic data shows the same broad magnetic features as seen in the ground survey, although the small individual targets have not been resolved due to the large sensor height. Three bullseye magnetic anomalies are evident within the Whyte River complex to the west of the ground survey. These are located on two weak northeast-trending magnetic lineaments. Although these also correspond to high conductivity, the geology in this area is unfavourable for carbonate-replacement mineralisation.

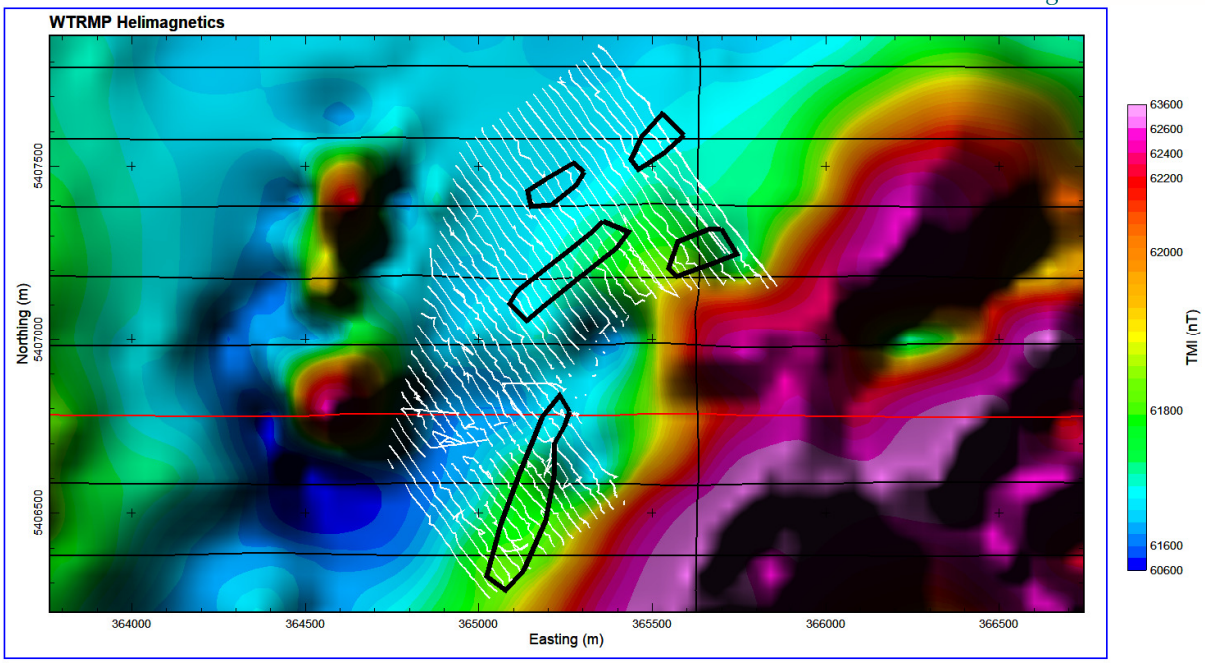

Figure 25 Grid of WTRMP helimagnetic data from Cleveland, sunshaded from the northeast. The ground magnetic survey lines are shown in white. The black polygons show the rough outlines of the five targets identified by Elementos (Figure 1). Flightline 10531 is highlighted in red.

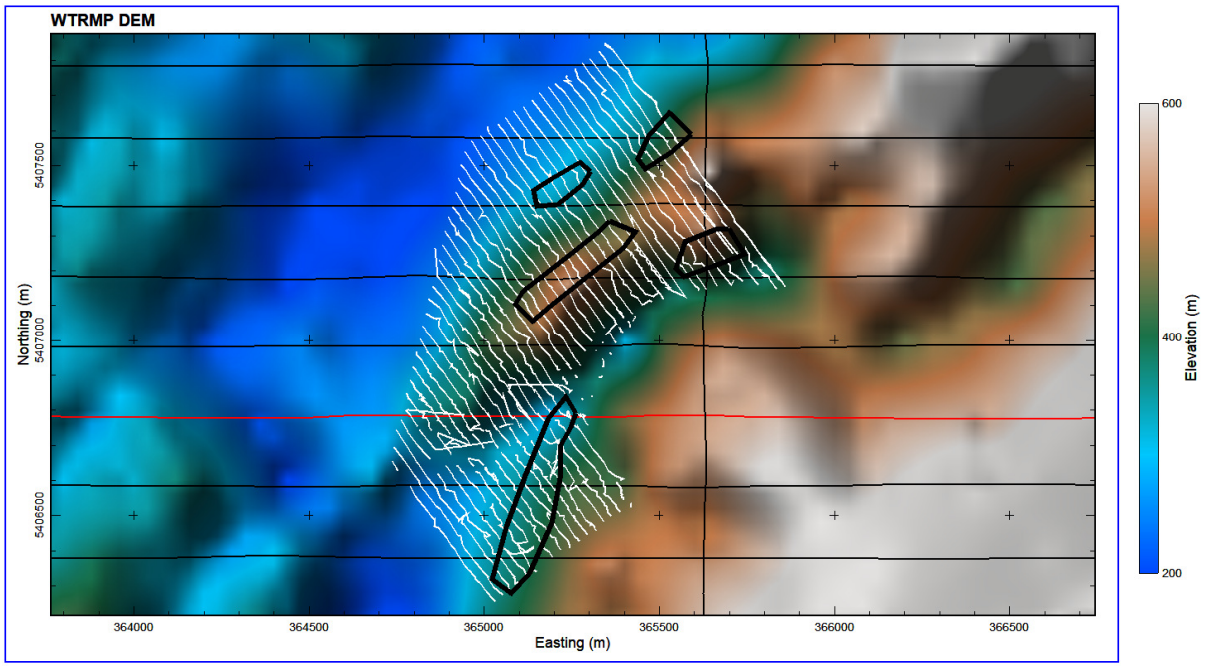

Figure 26 Grid of WTRMP digital elevation model from Cleveland. The ground magnetic survey lines are shown in white. The black polygons show the rough outlines of the five targets identified by Elementos (Figure 1). Flightline 10531 is highlighted in red.

Figure 27 shows profiles of selected Hummingbird data from Line 10531, which crosses the weak conductor at the northeastern end of the dyke target. There is only a very weak, broad anomaly evident at the approximate location of the conductor in Figure 25 (365175E), and at 880 Hz it is only present in the quadrature component. This further suggests that the anomaly is due to weakly conductive cover rather than pyrrhotite mineralisation. The strong response associated with the Whyte River complex is centred at ~364600E.

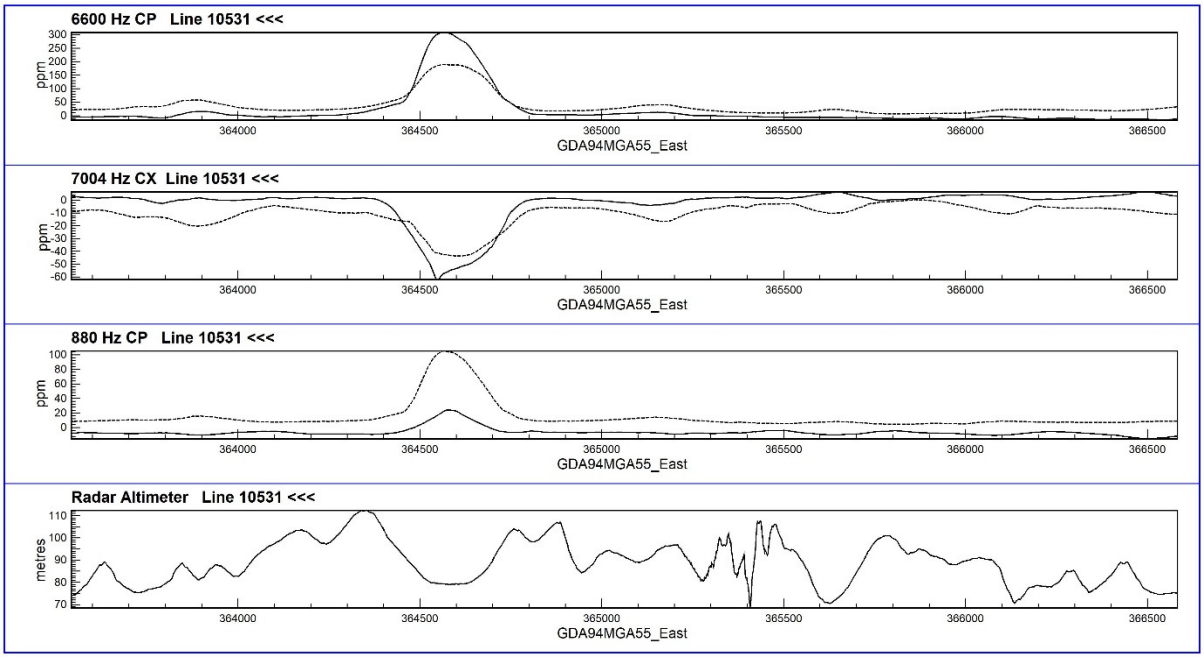

Figure 27 Profiles of 6600 Hz CP (top), 7004 Hz CX (second top), 880 Hz CP (second bottom), and Radar Altimeter (bottom). The radar altimeter gives the helicopter altitude. The EM system is towed approximately 30 m beneath the helicopter. In the upper three panels, the inphase response is shown as solid lines and quadrature as dashed lines.

6. Conclusions

Magnetic response associated with possible targets identified by Elementos has been assessed. Magnetic modelling has been completed to produce 3D models for all the selected targets except for target #4 (discussed below). Hummingbird AEM data over the survey area was also assessed. There were no EM anomalies within the extents of the ground magnetic survey that warranted plate modelling, but the review of the AEM data has been documented in this report.

6.1. Magnetic modelling

Magnetic modelling used a combination of profile modelling using Windisp, and full 3D magnetic using Gocad Mining Suite and VPmg software.

In overview, depths of all modelled domains were generally within the top 20m with only localized portions occurring at depths greater than this. Dips of modelled domains were generally close to vertical, but did vary from target to target (e.g. Target # 3 was modelled with a slight dip towards the north). The shallowest dip was for the SW body associated with Target #1 which was at 60 degrees. Magnetic modelling is relatively insensitive to depth extent of the domains when the depth to top is significantly less than the depth extent. This is the reason why most major domains have a similar depth extent – that is, there was no benefit to the data fit adjusting it from the starting value.

It is important to recognise that the supplied models are not unique, but are 3D interpretations of the magnetic data. The depth to the top of the bodies is reasonably well controlled by the wavelength of the magnetic signatures, but the inferred dip may be affected by superposition of nearby magnetic features, the removal of regional (background) geology, data quality, and even magnetic remanence. Putting these aspects aside, the sensitivity of the computed model responses to varying dip is continually gauged during interpretation and modelling of these domains. Based on this insight, our estimate on the accuracy of the modelled dip values is ~ +/- 10 degrees.

A known dyke to the south of the ground magnetic survey was included in the modelling with a view to assessing irregularities along the strike of the dyke. Irregularities were noted within this report from assessment of the data itself, and the modelled wireframes for the dyke.

Although Target #4 was the focus of various investigations, wireframe modelling was not completed for this target. The presence of a positive magnetic anomaly was questionable and

noise effected data across the topographic ridge was a concern. A reverse polarity (negative) magnetic anomaly exists across the top of the ridge and could be modelled if reverse polarity magnetic remanence were considered.

As agreed, it was assumed that magnetic remanence and self-demagnetisation could be ignored during magnetic modelling in this project. Given the range of magnetic susceptibilities used for modelling, the assumption to ignore self-demagnetisation is valid.

In terms of magnetic remanence, it needs to be stated that the presence of magnetic remanence (not aligned with the inducing field) may alter inferred dips from the modelling. Without sufficient control on either the magnetic susceptibility, model geometry (or both), this ambiguity will always exist in the modelling. In the absence of any additional information it is common to ignore magnetic remanence during preliminary modelling exercises. For the anomalies that were modelled in this project (except possibly with the exclusion of Target #4), there was no evidence to suggest that magnetic remanence was adversely affecting the results.

One of the challenges to this modelling exercise was data quality, primarily due to rugged terrain (particularly when the anomaly of interest was sometimes only 10s of nanoTeslas).

It was evident from inspection of the supplied magnetic database that some bad measurements had already been removed. Specific issues noted in the data by Mira included:

- Remaining spikes/outliers in the data.
- Repeat lines in the data that were not consistent.
- Erratic GPS height readings.

During modelling, spurious outliers or inconsistent lines were removed as required. Given the circumstances with the data acquisition, it is important to recognise the possibility that less conspicuous spurious anomalies may still exist in the data set. The entire data set was not re-processed or cleaned, bad data was simply removed as required to facilitate modelling.

6.2. AEM outcomes

No strong Hummingbird conductors likely to be associated with pyrrhotitic mineralisation were evident within the Area of Interest. It is likely that the remaining lenses of pyrrhotite-cassiterite mineralisation are too small to be resolved by airborne electromagnetic methods, or that the sulphide contents are too low to make the mineralisation strongly conductive. Greater

than ~5 wt% pyrrhotite (or other conductive sulphide) would be required to significantly increase the conductivity.

7. Recommendations

Our primary recommendation is to make the most of the modelling results to assist planning of drill holes, but to be aware of the non-uniqueness associated with magnetic modelling. If initial drilling does not corroborate the modelling, this should not be considered a failing of the method, rather an opportunity to understand what was overlooked in the first place.

Collection of rock property measurements is recommended during ongoing exploration. Particularly, if continued magnetic modelling is considered constraints on magnetic susceptibility and magnetic remanence would serve to reduce ambiguity in the interpretation and modelling of magnetic data.

For this project, there were no subsurface constraints (geological or petrophysical) available, and it is not even certain whether the magnetic responses over the nominated targets are associated directly with pyrrhotite, skarn alteration, dykes or other. Forward modelling of known mineralization wireframes and any associated alteration can serve to better characterize the geophysical signatures of targets.

There is scope for reconciling differences between the GPS elevation data of the ground magnetic survey and the LIDAR. Putting aside the average difference between the two, coherent deviations in GPS elevation from the LIDAR may need to be reconciled if the modelled wireframes are to be returned to the same datum as the GPS elevation data.

It is recommended that petrophysical electrical conductivity measurements be conducted on a few samples of the mineralization (at varying grades). Should the mineralisation prove to have significant conductivity, shallow surface frequency-domain electromagnetic surveys (e.g., EM34 or MaxMin) may be possible in the area. Unlike time-domain surveys, frequency-domain techniques do not require large square or rectangular transmitter loops, which would be unfeasible in the terrain around Cleveland.

Understand and develop a 3D geological model of the area. This would not only be a strong driver for exploration, but would directly assist in separating geological background magnetic response from response directly associated with potential targets. At a more regional scale, a review of the geology will also serve to corroborate the possible EM/mag targets to the west (which are assumed to be in unfavourable geology for carbonate-replacement mineralisation).

References

Fullagar, P.K., Hughes, N., and Paine, J., 2000, Drilling-constrained 3D gravity interpretation, Exploration Geophysics, 31, 17-23.

Fullagar, P.K., Pears, G.A., Hutton, D., and Thompson, A, 2004, 3D gravity & aeromagnetic inversion, Pillara region, W.A., Exploration Geophysics, 35, 142-146.

Fullagar, P.K., and Pears, G.A., 2007, Towards geologically realistic inversion: Proceedings of Exploration '07, Fifth Decennial International Conference on Mineral Exploration, Toronto.

Fullagar, P.K., Pears, G.A., and McMonnies, B., 2008, Constrained inversion of geological surfaces - pushing the boundaries: The Leading Edge, 27, 98-105.

Emerson, D. W., Martin, K., and Williams, P. K., 1999, Electrical, magnetic and mass properties of the nickeliferous komatiite sequence near Leinster, WA: ASEG Preview, **81**, 13-22.

Emerson, D. W., Williams, P. K., and Luitjens, S., 2001, The conductivities of Komatiitic Nickel Ores at Kambalda, WA: ASEG Preview, **92**, 38-41.

Reid, J., 2003, Western Tasmanian Regional Minerals Program, Helicopter electromagnetic data — Processing, quality control and interpretation, Part 3: Regional interpretation, Meredith Granite: Mineral Resources Tasmania, Tasmanian Geological Survey Record 2003/09.

Morrison, K. C., Reed, A. R., and Turner, N. J., 2003, Western Tasmanian Regional Minerals Program, Devonian Granite Aureoles Project Regional map set and geophysical signatures of major deposits: Mineral Resources Tasmania Tasmanian Geological Survey Record 2003/13.

Appendix: Digital deliverables.

The following digital deliverables are provided:

- This report.
- 3D DXFs of the modelled wireframes.
- DXF of the map view representation of cross-section locations shown in this report.
- DXF of the model depth slices shown within this report.
- Ascii data of the measured and calculated responses of models.
- Ascii data of the regional trend removed data.
- A Geoscience ANALAYST project comprising the models and computed responses.

Geoscience ANALYST can be downloaded from the Mira Geoscience website (see link below).

http://www.mirageoscience.com/our-products/software-product/geoscience-analyst

The viewer is free, but registration for a license is required.

All data was provided in a GDA94 (metric co-ordinate system), and digital deliverables are returned in the same co-ordinate system that the data was provided in.

It is important to note that magnetic data were positioned 1.5m above the supplied LIDAR topography for magnetic modelling, due to irregularities in the GPS elevations. The wireframes and associated deliverables are therefore positioned relative to the LIDAR DEM.

Appendix: VPmg Software

VPmg is a gravity, gravity gradient, magnetic, and magnetic gradient 3D modelling and inversion program developed by Fullagar Geophysics Pty Ltd (Fullagar et al., 2000; Fullagar et al., 2004; Fullagar and Pears, 2007; Fullagar et al., 2008).

In VPmg, the models are geological (categorical) in so far as each volume of the subsurface is assigned to a rock unit. The shape and property (density or susceptibility) of each unit can change during inversion, but its geological (or topological) identity is preserved. Geological contacts can be fixed (where pierced by a drill hole for example), bounded, or free to move during inversion. Bounds can be imposed on each unit's properties, and density or susceptibility measurements (on drill core samples or from downhole logs) are honoured during property inversion.

VPmg represents the sub-surface as a set of tightly -packed vertical rectangular prisms, which in plan view appear as a regular mesh or grid. Prism tops honour surface topography, and in its simplest form, internal contacts representing geological boundaries divide each prism into (usually elongated) cells. The vertical dimension of cells is arbitrary, implying that the vertical position of the geological boundaries is not "quantised" by vertical discretisation. The internal contacts represent geological boundaries that collectively define the shape of geological units. The geological units can either be homogeneous, i.e. uniform in density or susceptibility, or fully heterogeneous. When considering property inversion, a geological unit can be discretised in different ways. In the first instance, the property of each vertical prism segment of a geological unit can be allowed to vary independently, thereby introducing a lateral property variation within the unit. Full 3D property variation is achieved by introducing vertical sub-celling within the selected units.

VPmg offers considerable flexibility during interpretation. The model complexity ranges from conventional (uniform density) terrain models, to discrete bodies in a uniform background, to layered stratigraphy on basement, to complex 3D models. Regional effects can be handled by constructing a regional model, based on a relatively large rectangular mesh. The regional model is in turn embedded in a uniform half-space. A local model, comprised of smaller prisms, can be embedded in a regional model. The local model parameters can be adjusted by inversion until the gravity, gravity gradient, TMI, or magnetic gradient data within the local model area are satisfied.

VPmg offers a variety of inversion styles: homogeneous unit property, contact geometry, and heterogeneous property. During property inversion, model contacts (geometry) are fixed.

During contact geometry inversion, geological boundaries are altered while physical properties remain fixed. The user is able to easily switch from one inversion style to another.

GOCAD Mining Suite utilities developed by Mira Geoscience facilitate communication of model and data information to and from VPmg, and expedite assignment of drill hole constraints.